70th International Astronautical Congress (IAC), Washington D.C., United States, 21-25 October 2019.

IAC-19-D2-6x50636

Wind Tunnel investigations in CALLISTO - Reusable VTVL Launcher First Stage Demonstrator

Ansgar Marwege[a]*, Johannes Riehmer[a], Josef Klevanski[a], Ali Gülhan[a], Etienne Dumont[b]

[a] *DLR, Institute of Aerodynamics and Flow Technology, Supersonic and Hypersonic Technologies Department, Linder Hoehe, 51147 Cologne, Germany, ansgar.marwege@dlr.de*
[b] *DLR, Institute of Space Systems, Robert Hooke-Str. 7, 28359 Bremen, Germany*

Abstract

In order to make access to space more affordable for both scientific and commercial activities the German Aerospace Center (DLR), the Japanese Aerospace Exploration Agency (JAXA), and the French National Centre for Space Studies (CNES) joined in a trilateral agreement to develop and demonstrate the technologies that will be needed for future reusable launch vehicles. In the joined project CALLISTO (Cooperative Action Leading to Launcher Innovation in Stage Toss back Operations), a demonstrator for a reusable vertical take-off, vertical landing rocket is being developed and built. The long-term objective of the project aims at paving the way to develop a reusable launcher first stage, and the joint efforts of the three agencies will culminate with CALLISTO demonstration flights from the Kourou Space Center in French Guyana.
The aerodynamic and aerothermal characteristics of the CALLISTO vehicle are investigated by DLR, including its challenging variety of configurations and large flight envelope with high angles of attack and subsonic, transonic and supersonic flight regimes. To cross-check the CFD data and for an enhanced understanding of the vehicle aerodynamics, a first test Champaign was performed in the Trisonic Wind Tunnel (TMK) at the DLR Department of Supersonic- and Hypersonic Flow Technologies in Cologne. Data has been generated for Mach numbers between 0.5 and 2.5. The experiments considered the ascent as well as the backwards orientated descent configurations of the vehicle with folded and deployed aerodynamic control surfaces at several deflection angles. The angle of attack was continuously varied for all configurations.
The measurements of force and moment coefficients demonstrated the trimmability, stability and controllability of the vehicle for the planar fins deflection angles of up to 20° for all tested Mach numbers. Furthermore, the dependency of the aerodynamic coefficients on the Mach number was analyzed. Roll moment measurements showed efficient controllability of the roll angle. Investigations with oil film technique gave insight in the boundary layer separation of the body and the fins.
This paper describes the tested configurations, the experimental methods and main results of the test campaign, focusing on the fin efficiency and on force measurements with tripping, including the subsonic regime.

Keywords: Wind Tunnel Tests, Aerodynamic Database, Reusable Launch Vehicle, Demonstrator

Nomenclature

Acronyms/Abbreviations

DLR	German Aerospace Center
CNES	French National Centre for Space Studies
JAXA	Japanese Aerospace Exploration Agency
TMK	Trisonic Wind Tunnel Cologne
CFD	Computational Fluid Dynamics
RLV	Reusable Launch Vehicle
VTVL	Vertical Take-off Vertical Landing

1. Introduction

Making access to space more affordable is the main objective of the trilateral agreement CALLISTO (Cooperative Action Leading to Launcher Innovation in Stage Toss back Operations) of the German Aerospace Center (DLR), the French National Centre for Space Studies (CNES) and the Japanese Aerospace Exploration Agency (JAXA). In this scope the development and demonstration of technologies needed for reusable future launch vehicles is indispensable. Hence, CALLISTO is developed and built as a demonstrator for a Vertical Take-off, Vertical Landing (VTVL) rocket, acting as a first stage. In the long run the common effort will lead to a flight vehicle, which will be tested during a flight campaign at the Kourou Space Center in French Guyana (see [1] and [2]).

The aerodynamic and aerothermodynamic behavior of the CALLISTO vehicle are investigated at DLR, including its challenging configurations with high angles of attack and subsonic up to supersonic flight regimes. To cross-check the aerodynamic data from CFD and for the enhancement of the understanding of the aerodynamic characteristics of the vehicle, experiments were performed in the Trisonic Wind Tunnel (TMK) at the DLR Department of Supersonic- and Hypersonic Flow Technologies in Cologne for Mach numbers between 0.5 and 2.5.

The experiments considered the ascent and the backwards orientated decent configurations of the vehicle with folded and deployed aerodynamic control surfaces. The angle of attack was continuously varied for all configurations.

The wind tunnel test series described in this paper was performed in several stages starting at the end of 2018. The results of the test series were presented in [3] focusing on the comparison with CFD, and in [4] focusing more in depth on the flow topology, boundary layer tripping and the comparison of roll moment measurements with Low Resolution Euler CFD. This paper will give an overview over the performed tests and will go into more detail on the fin efficiency and on force measurements with boundary layer tripping devices, including the subsonic regime.

2. Trisonic Wind Tunnel TMK at DLR Cologne

The experiments presented in this paper were carried out in the Trisonic Wind Tunnel (TMK) at the DLR in Cologne. The TMK is a blow down wind tunnel with a Mach number range of $0.5 < Ma < 5.7$, and with a rectangular 0.6 m x 0.6 m test section. It is sketched in Fig. 1. Compressed air from a pressure reservoir passes a storage heater, a settling chamber, a Laval nozzle, a test section and a diffuser. With the volume of the pressure reservoir of 1000 m^3 at a pressure of up to 60 bar, test durations of up to 60 seconds can be reached. During supersonic tests, the Mach number is controlled via the adaptable nozzle; for the transonic and subsonic regime it is controlled with the diffuser. The wind tunnel model is fixed in the test section on a motion control device, with which the incident angle of the model can be controlled. Due to the adaptable nozzle and the motion control device, α-polars can be run for several Mach numbers in one run. In the transonic and subsonic regime, only one Mach number per run can be tested.

The wind tunnel is operated at a static pressure of $p_\infty \approx 1\ bar$ for Mach numbers $Ma < 1.2$, and at a constant dynamic pressure $q_\infty \approx 1\ bar$ for higher Mach numbers ($Ma > 1.2$) . Up to Mach 5.7 can be reached by heating the air in the storage heater and by the use of an ejector downstream of the diffuser. Due to the constant static pressure for $Ma < 1.2$, the dynamic pressure and, hence, the Reynolds number increases with increasing Mach numbers. The Reynolds numbers in this regime range from $Re = 1.2 \times 10^7\ m^{-1}$ ($Ma = 0.5$) to $Re = 3.7 \times 10^7\ m^{-1}$ ($Ma = 1.2$). For supersonic conditions, the Reynolds number can be varied in a range of $2.6 \times 10^7\ m^{-1} < Re < 7.6 \times 10^7\ m^{-1}$ by variation of the stagnation pressure (up to $p_0 = 25\ bar$) and temperature (up to $T_0 = 550\ K$). The Reynolds number variation can be extended by the use of the ejector.

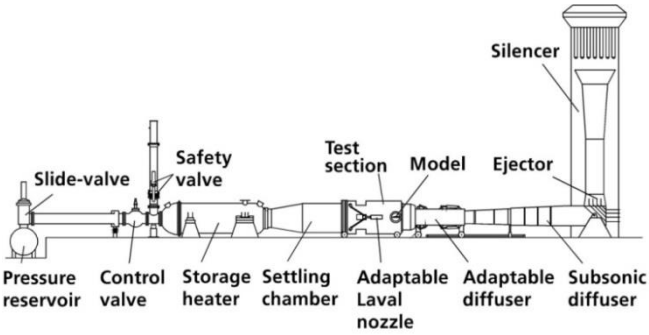

Fig. 1. Schematic of Trisonic Wind Tunnel TMK

For transonic and subsonic tests a test section with perforated walls is installed downstream of the supersonic test section. By variation of the aperture of the perforations, the boundary layer suction can be adapted to the flow conditions. The supersonic test section is equipped with large glass windows, which allow for investigations with schlieren technique in the supersonic regime. Due to the perforated walls installed for the subsonic and transonic regime, schlieren imaging cannot be performed for these tests.

The Mach number range of the TMK is supplemented by the Hypersonic Wind Tunnel (H2K), where Mach numbers of up to $Ma = 11.2$ can be tested. Due to compatible model adapters of the two wind tunnels, the same wind tunnel models can be used in both facilities. The facilities are described more in detail in [5] and [6].

Fig. 2 shows the open test section of the TMK; the performance map of the facility is shown in Fig. 3.

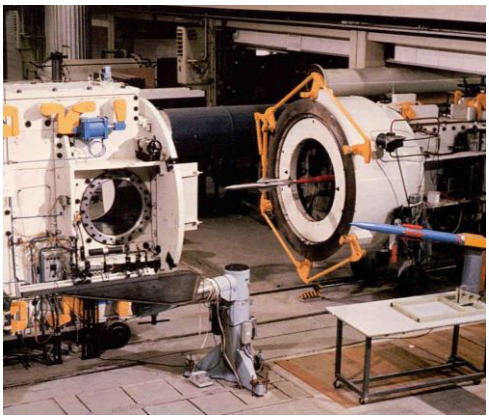

Fig. 2. Supersonic test section of Trisonic Wind Tunnel TMK

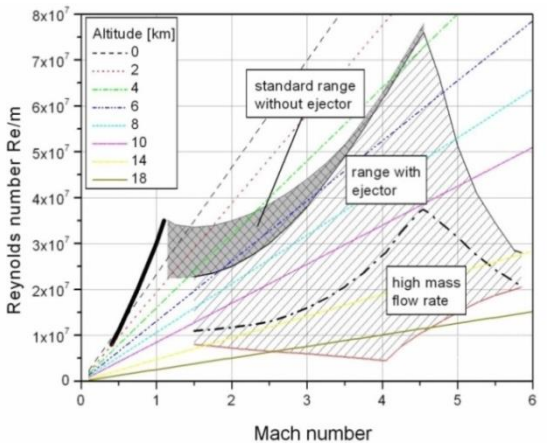

Fig. 3. Performance map of Trisonic Wind Tunnel TMK

3. Wind Tunnel Model and test procedure

Even though the test procedure was partly laid out in the precursor papers [3] and [4], it will be summarized in the following for the sake of completeness, showing the overall picture of the test series.

3.1. Tested Configurations

As described in [1] and [3], the main goal of CALLISTO is the demonstration of a "toss-back" flight profile with the following flight phases:

- Ascent phase (comparable to expendable launchers)
- "Tilt-over" manoeuvre
- "Boost back" phase
- Aerodynamic guided approach phase
- Landing boost and touchdown

In the first series of wind tunnel experiments, the flight phases without active engines are investigated which are the ballistic ascent phase and the aerodynamic guided approach of CALLISTO. The configurations for these phases (FFN and UFN) are shown in Table 1.

Configuration		Phase Applicable	Fins	Landing Legs	Thrust Plume
FFN (C1)		Ballistic MECO#1 – Fin Deploy	Folded	Folded	No Thrust Plume
UFN (C2)		Ballistic: Fin Deploy – MEIG#2 *and* Aerodynamic Descent: MECO#2 – MEIG#3	Unfolded (Deployed)	Folded	No Thrust Plume

Table 1: CALLISTO Configurations [7]

3.2. Reference Shape

The reference shape used for the wind tunnel experiments is the references shape CAL1B. It does not include protuberances like fuel lines, cable ducts etc. and it was the reference shape from which the first version of the Aerodynamic Data Base (AEDB) was computed. It is shown in Fig. 4.

Fig. 4. Reference shape CAL1B [7]

3.3. Model Scale and Design

Based on the reference shape, a model with a scale of 1/35 was built. The scaling was chosen to minimize blockage of the wind tunnel. The model is mounted on a biconical sting, which is then mounted on the motion control device of the α-drive. A sketch of the wind tunnel model for the FFN and the UFN configuration mounted on the sting can be seen in Fig. 5.

The wind tunnel model consists of various modules. This way, the forward facing FFN configuration ($\alpha = 0° \dots 20°$) and the backwards facing UFN configurations ($\alpha = 180° \dots 160°$) can be tested with the same model. Furthermore, several deflection angles of the planar fins can be tested. The modules of the model are shown in Fig. 6. The model mounted on the sting in the wind tunnel is shown in Fig. 7. Note that the configuration shows a step in the diameter, due to the insulation of the cryogenic tanks (see Fig. 5 and Fig. 7a).

The modules of the forward facing FFN configuration are: sleeve, center body, folded legs, complete nose for FFN, folded fins and a cover for the back part of the model. In this configuration the base of the model is open, as the sting is introduced in the model from this part (see Fig. 7a). The backward facing UFN configuration consists of: sleeve, center body, folded legs, a cover representing the engine of the vehicle, unfolded fins and a cut nose. There are three versions of the module of the unfolded fins for the three deflection angles $\delta = 0°,\ 10°, 20°$. In this configuration the sting is introduced from the nose in the model (see Fig. 5b and Fig. 7b).

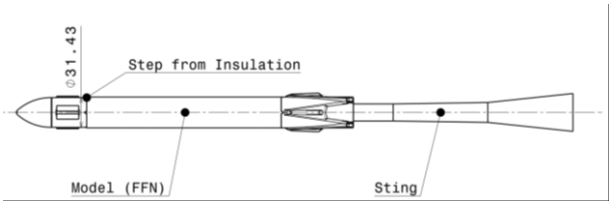

a) FFN

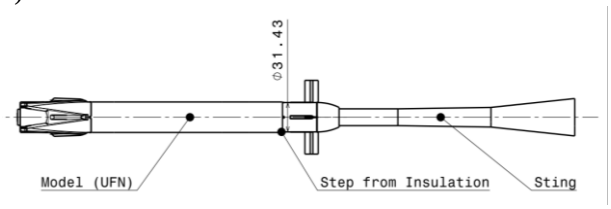

b) UFN

Fig. 5. Dimensions of the Model for the FFN and the UFN configuration

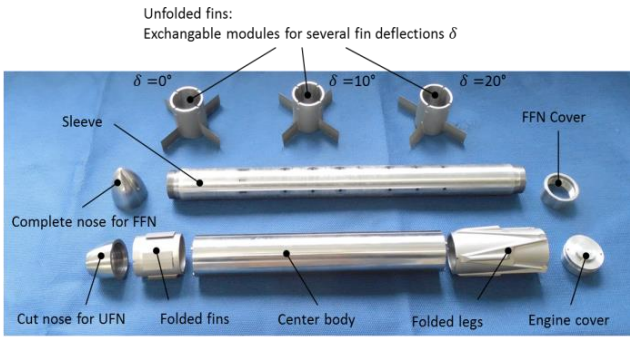

Fig. 6. Modular Wind Tunnel Model

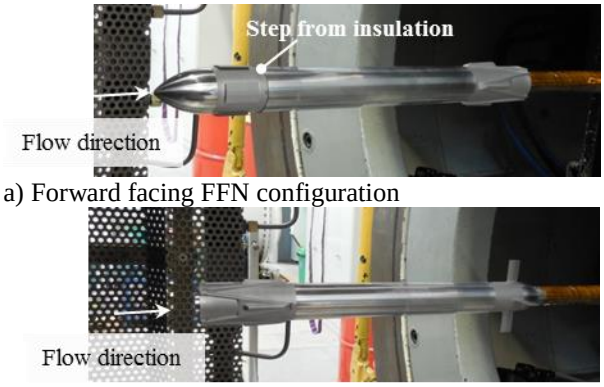

a) Forward facing FFN configuration

b) Backward facing UFN configuration

Fig. 7. Model mounted in the Trisonic Wind Tunnel (TMK)

3.4. Reference Frame

The forces and moments were measured in a coordinate system fixed to the balance. It is shown in Fig. 8a. However, the data has been transformed to the coordinate system used in the Aerodynamic Data Base (AEDB), which is shown in Fig. 8b. For comparability of results in both reference frames, the origin of the balance fixed reference frame was positioned on the tip of the nose of the model. Hence, for the UFN configuration, due to its cut nose, the origin lies outside the model in an imaginary nose tip.

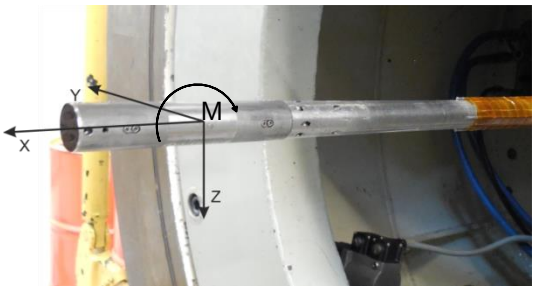

a) Balance fixed reference frame

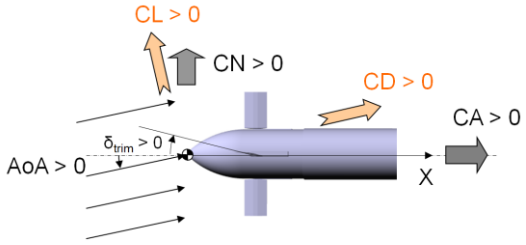

b) Reference frame used in AEDB

Fig. 8. Basis Fixed Coordinate System

The UFN configuration is investigated in a + and a X positioning. This refers to the position of the fins with respect to the angle of attack. In the + positioning the axis of rotation of the fins is parallel to the axis of the pitch rotation. In the X positioning the vehicle is turned by 45° around the x axis in comparison with the + positioning. The X and the + position are sketched in Fig. 9.

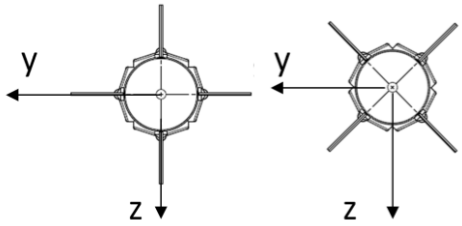

Fig. 9. Sketch of the + and X positioning of the vehicle

3.5. Model Instrumentation

For the static force and moments measurements the model was equipped with a six component strain gauge floating frame balance *Task 0.75"*. This balance was selected after a trade-off between the feasible axial load and the ratio of the model to sting diameter. The floating frame design leads to small contact areas of the balance and the model, which is why these balances yield high accuracies.

3.6. Test Procedure

A typical run of α over the time is shown in Fig. 10. First a slight down-sweep is performed to -3°. This way, the following up-sweep runs with a constant sweep velocity of 2°/s while passing $\alpha = 0°$. The up-sweep is performed up to a maximum angle of attack. In the position of maximum angle of attack the model is hold. Then, a down-sweep to 0° is performed. The data is evaluated for the main up- and the main down-sweep. This way, hysteresis effects can be analyzed. The data is filtered with a 2 Hz low-pass filter in the post-processing.

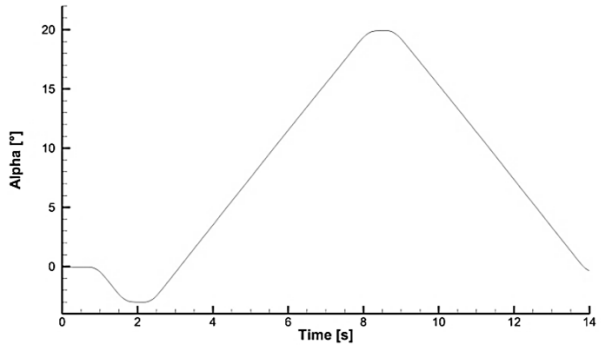

Fig. 10: Typical α over time

3.7. Matrix of Performed Tests

Table 2 shows the configurations and flow conditions of the performed tests. The tests included subsonic up to supersonic flow conditions for the FFN and UFN configurations described in Table 1. The fin deflection angles of $\delta = 0°, +10°, -10°, +20°, -20°$ were tested.

For Mach number 1.1 and 0.9 the blockage of the wind tunnel can get critical. High loads occurred for the balance for Mach 1.1 for $\alpha > 15°$. Therefore, for this Mach number the angle of attack was limited to 15° (165° for UFN configurations). For most configurations for supersonic conditions, angles of attack of higher than 20° (less than 160° for UFN configurations) could be run. For consistency of the data base of the WTT data, it was limited to 20° for all cases except for the Mach 1.1 case which was limited to 15°.

Further studies were performed with boundary layer tripping devices to study the influence of laminar-turbulent boundary layer transition on the force and moment coefficients. Silicon carbide tripping grains were applied to the fins on a length of 2.5 mm for $\delta = 0, -10°, +10°$ for the Mach numbers 0.5 to 0.7 and 1.5 to 2.5 (see Fig. 11). Tripping was also applied on an area of a length of 20 mm on the center body (see Fig. 12), were delamination of the flow from the center body due to shocks emerging from the folded landing legs could be expected. Typical grain sizes of F 80 (~150µm), F 220 (~45µm) and F 320 (~37µm) were used after a preliminary boundary layer assessment. Applying the model scaling to the grain size would result in perturbations in the order of 5.25 mm (F 80), 1.56 mm (F 220) and 1.3 mm (F 320) for the full flight configuration. In this paper only the boundary layer tripping on the fuselage will be discussed, as the tripping experiments in the subsonic regime for the fins are still ongoing.

Roll moments were measured for a deflection of $\delta = 10°$ for all fins for the Mach numbers 0.5 to 0.7 and 1.5 to 2.5.

Table 2: Matrix of performed tests

Ma	Model	Defl. δ [°]	q_∞ [bar]
0.50	FFN	-	0.18
0.70	FFN	-	0.37
0.90	FFN	-	0.61
1.10	FFN	-	0.93
1.50	FFN	-	0.90
2.00	FFN	-	0.96
2.50	FFN	-	0.94
0.50	UFN	0	0.19
0.70	UFN	0	0.37
0.90	UFN	0	0.60
1.12	UFN	0	0.94
1.50	UFN	0	0.91
2.00	UFN	0	0.97
2.50	UFN	0	0.94
0.50	UFN	+10	0.19
0.70	UFN	+10	0.37
0.90	UFN	+10	0.61
1.11	UFN	+10	0.92
1.50	UFN	+10	0.91
2.00	UFN	+10	0.97
2.50	UFN	+10	0.94
0.50	UFN	-10	0.19
0.70	UFN	-10	0.37
0.90	UFN	-10	0.61
1.11	UFN	-10	0.92
1.50	UFN	-10	0.91
2.00	UFN	-10	0.97
2.50	UFN	-10	0.94
0.50	UFN	+20	0.19
0.70	UFN	+20	0.37
0.90	UFN	+20	0.61
1.11	UFN	+20	0.92
1.50	UFN	+20	0.91
2.00	UFN	+20	0.97
2.50	UFN	+20	0.94
0.50	UFN	-20	0.19
0.70	UFN	-20	0.37
0.90	UFN	-20	0.61
1.11	UFN	-20	0.92
1.50	UFN	-20	0.91
2.00	UFN	-20	0.97
2.50	UFN	-20	0.94

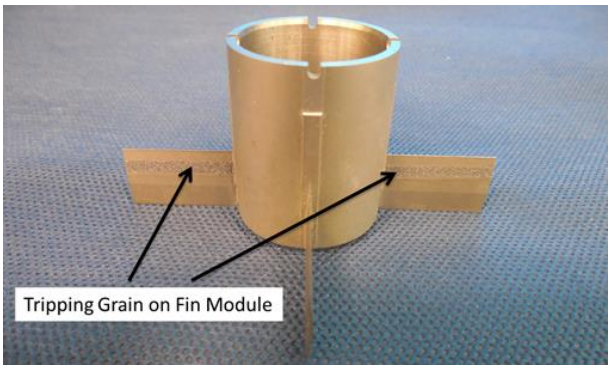

Fig. 11. Fin module with tripping grains

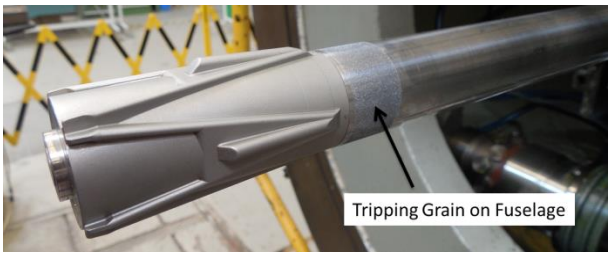

Fig. 12. Center body with tripping grains

4. Results

In the following, the detailed test results of the force and moment measurements are presented for the UFN configuration . For the moment coefficient CM based on the center of gravity (CoG), the position of the center of gravity was assumed as 60% of the length of the model from the nose tip of the model ($x_{tip} = 0\,mm$, see Fig. 8b).

No base pressure correction is implemented for CA as the model is not closed at the back side where the sting is introduced and hence the pressure inside the model can be assumed to be equal to the base pressure. Therefore, a pressure correction is not necessary.

4.1. Efficiency of the planar fins

In this section the UFN + configurations are compared for Mach 2.5, 2.0, 1.5, 1.1, 0.9, 0.7 and 0.5. For the supersonic regime a clear effect of the deflection of the control surfaces on CM (CoG) is visible. For Mach 0.9 the deflection of $\delta = -20°$ does not lead to higher CM (CoG) in comparison to $\delta = -10°$. The efficiency of the fins is saturated, probably due to stall on the fins. Also for Mach 0.7 and 0.5 a saturation of the fin efficiency at $\delta = -10°$ can be observed.

For a positive CM (CoG) for $\alpha < 180°$ and zero at $\alpha = 180°$ the UFN configuration will return to $\alpha = 180°$ and is statically stable for the backward flight. The center of gravity at 60% of the vehicle length

is a conservative assumption as, due to the fuel consumption, it will constantly move further backwards (moving away from the nose tip) during descent and therefore increase the stability of the backward flying configuration.

For the given position of the center of gravity the vehicle can be trimmed safely for a range of angles of attack $160° < \alpha < 180°$ for all tested Mach numbers. The necessary trim deflection is mainly less than $|\delta| = 10°$.

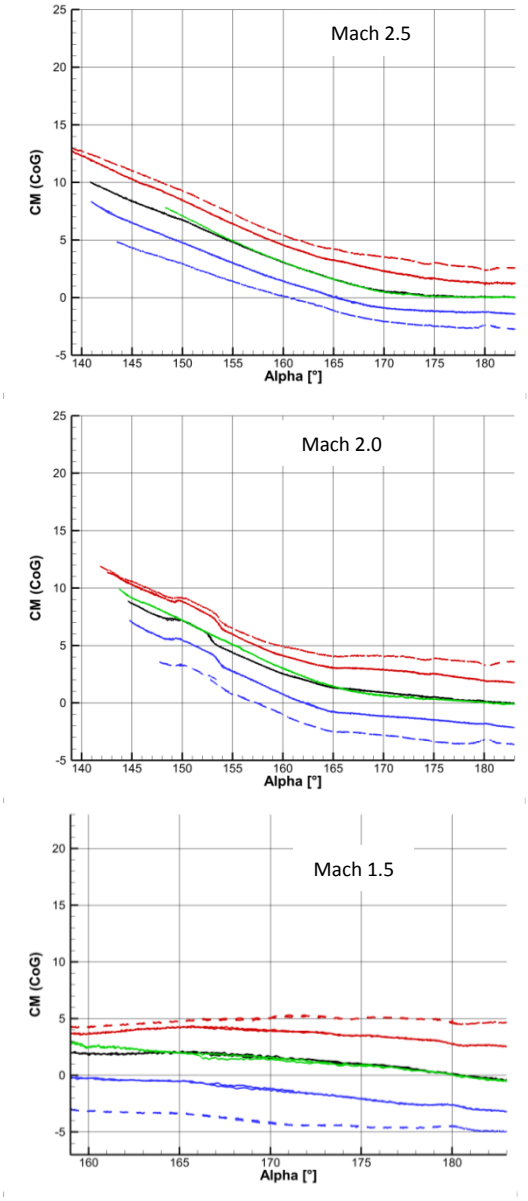

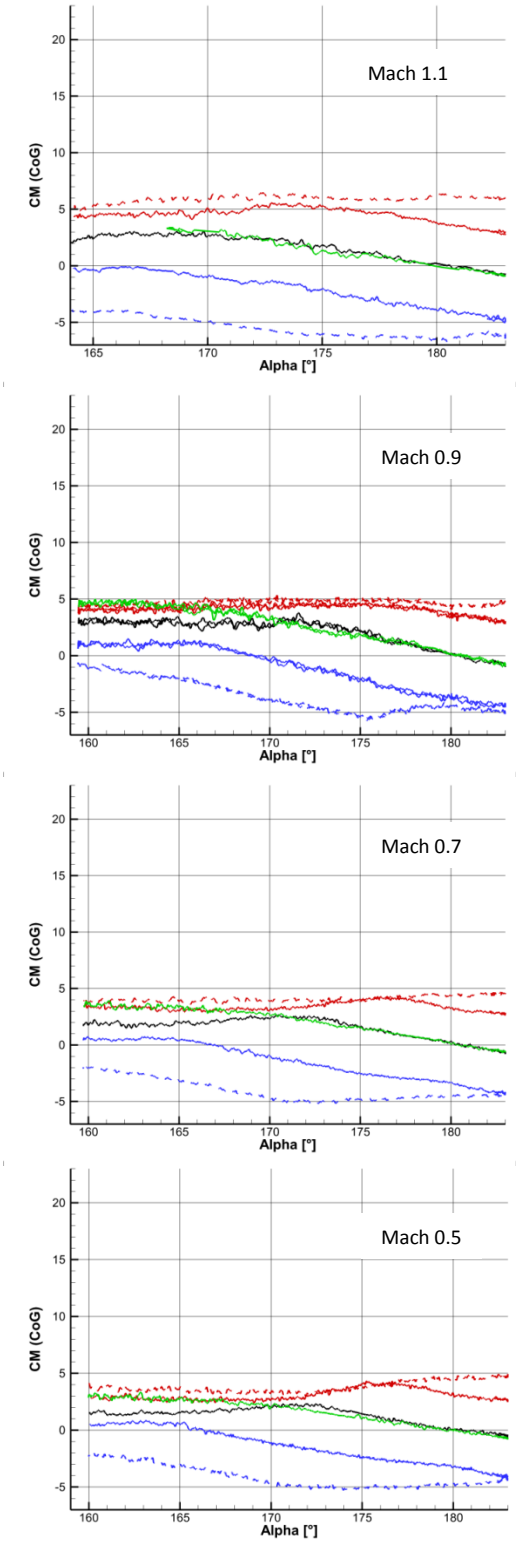

Fig. 13. Comparison of Moment coefficients for the UFN configurations of CALLISTO with:
— UFN +0, — UFN +10, - - - UFN +20,
— UFN -10, - - - UFN -20, — UFN x0

Fig. 14b shows the comparison of the UFN configurations for Mach 2.0. For all + configurations there is a irregularity in CN and CM (CoG) between$153° \lesssim \alpha \lesssim 149°$. As the irregularity occurs at roughly the same angle of attack for all UFN configurations, the reason for it has to come from the body and not from the fins. As it does not occur for the X configuration but only for the + configuration, it seems likely that it originates from the landing legs as they are turned by 45° from the + to the x configuration.

Fig. 15 shows the normal force coefficient for the UFN configurations of CALLISTO. In general at high angles of attack the efficiency of the fins decreases. However, this strongly depends on the Mach number. The efficiency decreases with decreasing Mach numbers. Especially at the Mach number 0.9 and below, the fins saturate at an angle of attack of about $\alpha = 170°$. As expected, a positive deflection of the fins is counteracted by the positive angle of attack. Therefore, the fins do not saturate for the positive deflections.

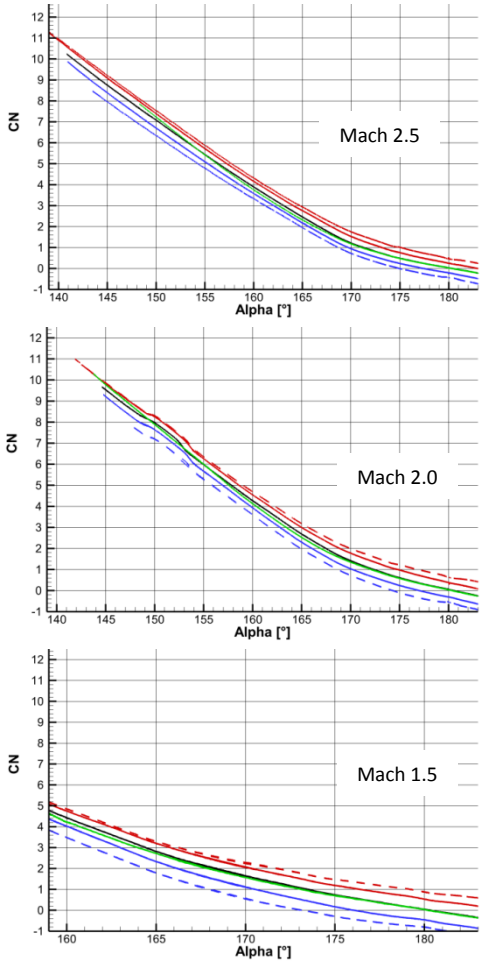

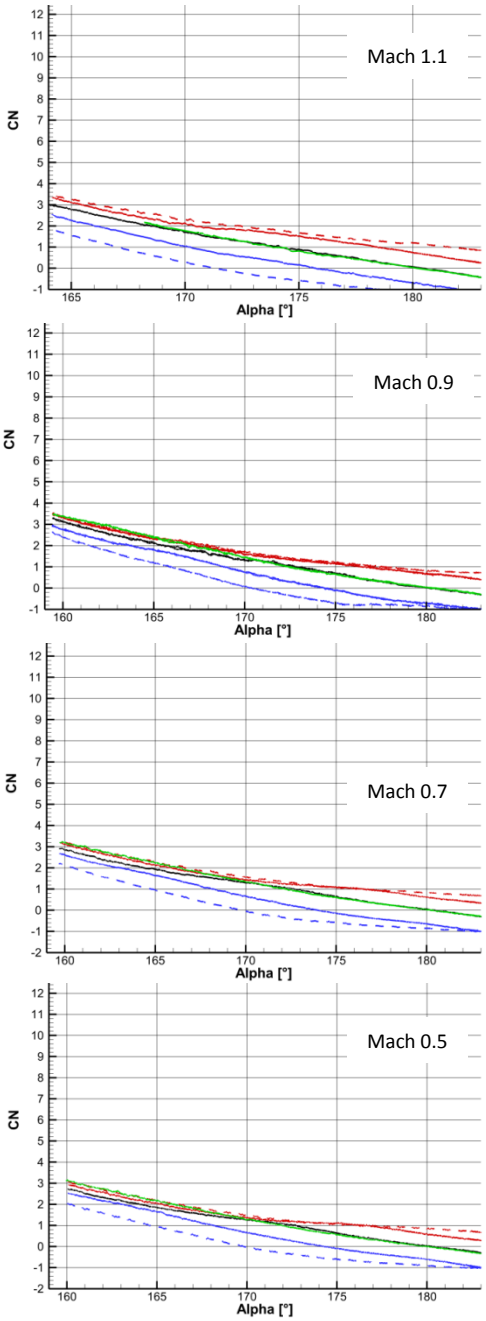

Fig. 15. Comparison of Normal Force coefficients for the UFN configurations of CALLISTO with:
— UFN +0, — UFN +10, - - - UFN +20,
— UFN -10, - - - UFN -20, — UFN x0

4.2. Boundary layer tripping

The boundary layer tripping in the supersonic regime was discussed in [4]. In Fig. 16 the results are shown for the subsonic regime for the Mach numbers 0.5, 0.7 and 0.9.

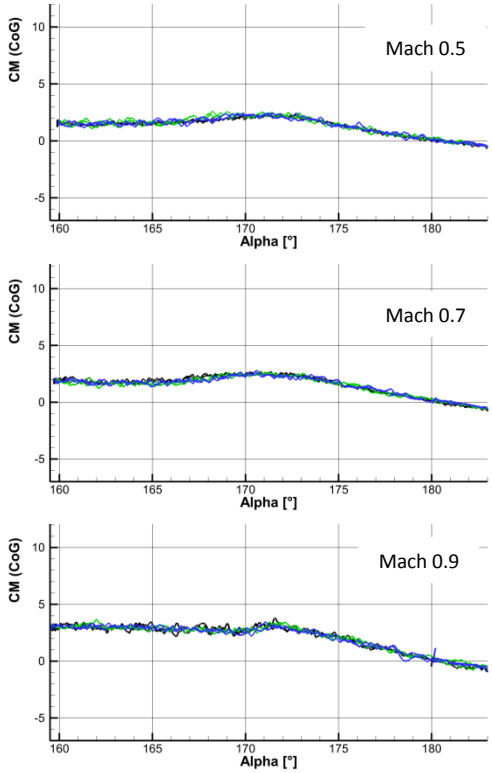

Fig. 16. Comparison of the moment coefficient in the assumed center of gravity for the UFN+0 configuration with and without boundary layer tripping on the body. (no tripping (black), F220 (green), F80 (blue))

The tripping grain has no remarkable effect on the moment coefficients. One possible reason is that the boundary layer on the fuselage can be expected to be turbulent even without tripping. Therefore the tripping does not greatly influence the flow field.

4.3. Roll moment measurements

In [4] the roll moments for the supersonic regime were already discussed. They are shown in Fig. 17 together with the roll moments for the subsonic regime. The roll moments in the subsonic regime depend less on the Mach number than the roll moments in the supersonic regime. However, a stronger dependence on the angle of attack can be observed. In the subsonic regime the polars follow the same shape and decrease constantly at angles of attack smaller than 176° (i.e. an increased effective angle of attack). Furthermore, while for the supersonic regime there is no clear trend for a difference between the roll moment for the + and the X configuration, this trend can be identified for the subsonic regime. While for the + configuration the roll moment coefficient constantly decreases up to high effective angles of attack (160°), a plateau is reached for the X configurations at approx. $\alpha = 165°$.

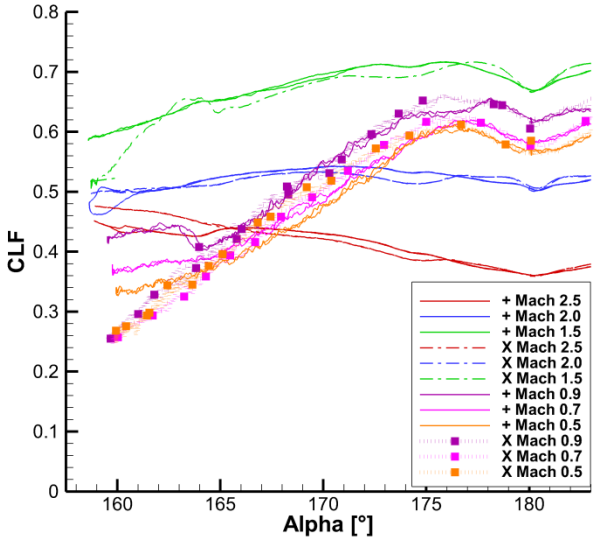

Fig. 17. Roll moment coefficients for the UFN configurations of CALLISTO.

5. Conclusions

Force measurements of the CALLISTO configuration were performed at the DLR Cologne in the TMK wind tunnel facility. The measurements give detailed insight in the aerodynamic behaviour of the vehicle. For an assumed position of the centre of gravity of the vehicle at 60% of the vehicle length from the nose tip, the vehicle can be trimmed safely for a range of angles of attack $160° < \alpha < 180°$ for all tested Mach numbers. The necessary trim deflection is mainly less than $|\delta| = 10°$. Boundary layer tripping was applied on the fuselage of the wind tunnel model. The measurements showed that it has no remarkable impact on the moment coefficient. Roll moment measurements in the subsonic regime showed, that the roll moment in the subsonic regime is less dependent on the Mach number. However, it depends stronger on the angle of attack. Also a stronger correlation of the roll moment with the flight configuration ("+" or "X") could be observed.

For a comprehensive understanding of the flight vehicle, further wind tunnel experiments with models with added protuberances (e.g. fuel lines, cable ducts) are foreseen in the frame of the CALLISTO project. The results of these will be presented in future publications.

Acknowledgements

The authors gratefully acknowledge the technical staff of the Trisonic Wind Tunnel (TMK), Martin Achner and Daniel Habegger, for their support and technical expertise.

References

[1] Dumont, E., Ecker, T., Chavagnac, C., Witte, L., Windelberg, J., Klevanski, J., Giagkozoglou. S. "*CALLISTO – Reusable VTVL launcher first stage demonstrator*", 2018, SP2018_00406. In: Space Propulsion Conference, 14-16 May, 2018, Sevilla, Spain.

[2] Dumont, E., Ishimoto, S., Tatiossian, P., Klevanski, J., Reimann, B., Ecker, T., Witte, L., Riehmer, J., Sagliano, M., Giagkozoglou, S., Petkov, I., Rotärmel, W., Schwarz, R., Seelbinder, D., Markgraf, M., Sommer, J., Pfau, D. and Martens, H. „*CALLISTO: a Demonstrator for Reusable Launcher Key Technologies*",32nd ISTS, 17-21. June 2019, Fukui, Japan.

[3] Marwege, A., Riehmer, J., Klevanski, J., Gülhan, A.,Ecker, T., Reimann, B., and Dumont, E. "*First Wind Tunnel Data of CALLISTO Reusable VTVL Launcher First Stage Demonstrator*", 8th European Conference for Aeronautics and Space Sciences, 1 – 4 July, 2019, Madrid, Spain.

[4] J. Riehmer, A. Marwege, J. Klevanski, A. Gülhan, E. Dumont, "*Subsonic and Supersonic Ground Experiments for the CALLISTO CTVL Launcher Demonstrator*", International Conference on Flight Vehicles, Aerothermodynamics and Re-entry Missions and Engineering (FAR) 30 Sept – 3 Oct, 2019, Milano, Italy.

[5] Esch, H. 1986. Die 0.6-m x 0.6-m – „*Trisonische Meßstrecke (TMK) der DFVLR in Köln-Porz (Stand 1986)*", DFVLR-Mitt. 86-21, Cologne. 1986

[6] Niezgodka, F.-J. Der „*Hyperschallwindkanal H2K des DLR in Köln-Porz (Stand 2000)*", DLR-Mitt. 2001-01, Cologne.DOI: 10.13009/ EUCASS2017-680, 2001

[7] Klevanski, J., Ecker, T., Riehmer, J., Reimann, B., Dumont, E., Chavagnace C. „*Aerodynamic Studies in Preparation for CALLISTO - Reusable VTVL Launcher First Stage Demonstrator*" 69th International Astronautical Congress (IAC), IAC-18-D2.6.3, 2018, Bremen, Germany.